5426 *Biochemistry* **2009,** *48,* 5426–5434
DOI: 10.1021/bi9001375

BIOCHEMISTRY
including biophysical chemistry & molecular biology
Article

Human Glyoxalase II Contains an Fe(II)Zn(II) Center but Is Active as a Mononuclear Zn(II) Enzyme†

Pattraranee Limphong,‡ Ross M. McKinney,‡ Nicole E. Adams,‡ Brian Bennett,§ Christopher A. Makaroff,‡ Thusitha Gunasekera,‡ and Michael W. Crowder*,‡

‡*Department of Chemistry and Biochemistry, 160 Hughes Hall, Miami University, Oxford, Ohio 45056, and* §*National Biomedical EPR Center, Department of Biophysics, Medical College of Wisconsin, Milwaukee, Wisconsin 53226*

Received January 28, 2009; Revised Manuscript Received April 19, 2009

ABSTRACT: Human glyoxalase II (Glx2) was overexpressed in rich medium and in minimal medium containing zinc, iron, or cobalt, and the resulting Glx2 analogues were characterized using metal analyses, steady-state and pre-steady-state kinetics, and NMR and EPR spectroscopies to determine the nature of the metal center in the enzyme. Recombinant human Glx2 tightly binds nearly 1 equiv each of Zn(II) and Fe. In contrast to previous reports, this study demonstrates that an analogue containing 2 equiv of Zn(II) cannot be prepared. EPR studies suggest that most of the iron in recombinant Glx2 is Fe(II). NMR studies show that Fe(II) binds to the consensus Zn_2 site in Glx2 and that this site can also bind Co(II) and Ni(II), suggesting that Zn(II) binds to the consensus Zn_1 site. The NMR studies also reveal the presence of a dinuclear Co(II) center in Co(II)-substituted Glx2. Steady-state and pre-steady-state kinetic studies show that Glx2 containing only 1 equiv of Zn(II) is catalytically active and that the metal ion in the consensus Zn_2 site has little effect on catalytic activity. Taken together, these studies suggest that Glx2 contains a Fe(II)Zn(II) center in vivo but that the catalytic activity is due to Zn(II) in the Zn_1 site.

The glyoxalase system consists of two enzymes, lactoylglutathione lyase (glyoxalase I, Glx1) and hydroxyacylglutathione hydrolase (glyoxalase II, Glx2) (*1*−*3*). Glx1 is capable of forming *S*-(2-hydroxyacyl)glutathione (SLG),[1] which is made from the thiohemiacetal produced from a spontaneous reaction of methylglyoxal and glutathione. SLG (and other related glutathione thiolesters) is then hydrolyzed by Glx2 to form D-lactate and glutathione. Glyoxalase I can utilize a number of α-ketoaldehydes; however, the primary physiological substrate of the system is thought to be methylglyoxal (MG), a cytotoxic and mutagenic compound that is formed primarily as a byproduct of carbohydrate and lipid metabolism and from triosephosphates (*2*, *4*−*6*). SLG is also cytotoxic because of its ability to inhibit DNA synthesis (*2*, *7*). While SLG can also be metabolized by γ-glutamyltransferase and dipeptidase, these processes generate *N*-D-lactoylcysteine, which also inhibits nucleotide synthesis (*7*). Therefore, the glyoxalase system, which depletes MG and SLG, plays a critical role in cellular detoxification (*1*, *8*).

Because of its role in cellular detoxification, the glyoxalase system has received considerable attention as a possible antitumor and antiparasitic target in animal systems (*1*, *9*−*18*). Increased levels of Glx1 and Glx2 mRNA and protein have been detected in tumor cells, such as in breast carcinoma cells, and glyoxalase inhibitors have been shown to inhibit the growth of tumor cells in vitro (*19*). Therefore, it has been proposed that the targeted inhibition of glyoxalase enzymes can be a viable anticancer strategy (*5*, *11*, *13*, *18*, *20*−*26*). *Plasmodium falciparum* and the protozoan *Leishmania* exhibit high rates of methylglyoxal formation and increased levels of Glx1 activity (*27*, *28*). In *Leishmania infantum*, trypanothione is used instead of glutathione, and a crystal structure of *L. infantum* Glx2 bound to *S*-D-lactoyltrypanothione has recently been reported (*29*).

Alterations in glyoxalase activity have also been associated with several other disease states. Glx1 and Glx2 can inhibit the

†This work was supported by the National Institutes of Health (Grant AI056231 to B.B., Grant GM076199-01A2 to C.A.M., and Grant EB001980 to the Medical College of Wisconsin), the Miami University/Volwiler Professorship (to M.W.C.), and a Presidential Academic Enrichment Fellowship (to P.L.).

*To whom correspondence should be addressed. E-mail: crowdemw@muohio.edu. Phone: (513) 529-7274. Fax: (513) 529-5715.

[1]Abbreviations: EDTA, ethylenediaminetetraacetic acid; FPLC, fast performance liquid chromatography; Glx2-Co_{min}, recombinant human glyoxalase II overexpressed in minimal medium containing Co(II); Glx2-Co_{min} + Zn(II), recombinant human glyoxalase II overexpressed in minimal medium containing Co(II) to which was added 1 equiv of Zn(II); Glx2-Fe_{min} + Zn(II), recombinant human glyoxalase II overexpressed in minimal medium containing Fe and Zn(II); Glx2-LB, recombinant human glyoxalase II overexpressed in LB medium; Glx2-LB + 1.5Zn + 1.5Fe, recombinant human glyoxalase II overexpressed in LB medium which was incubated with 1.5 equiv of Zn(II) and Fe(II) and dialyzed; Glx2-Zn_{min}, recombinant human glyoxalase II overexpressed in minimal medium containing Zn(II); Glx2-Zn_{min} + Ni(II), recombinant human glyoxalase II overexpressed in minimal medium containing Zn(II) to which was added 1 equiv of Ni(II); Glx2-Zn_{min} + 3equivFe(II), recombinant human glyoxalase II overexpressed in minimal medium containing Zn(II) which was incubated with 3 equiv of Fe(II) and dialyzed; Glx2-Zn_{min} + 3equivZn(II), recombinant human glyoxalase II overexpressed in minimal medium containing Zn(II) which was incubated with 3 equiv of Zn(II) and dialyzed; HEPES, 4-(2-hydroxyethyl)-1-piperazineethanesulfonic acid; ICP-AES, inductively coupled plasma with atomic emission spectroscopy detection; IPTG, isopropyl β-D-thiogalactopyranoside; LB, Luria-Bertani; MG, methylglyoxal; MOPS, 3-morpholinopropanesulfonic acid; PMSF, phenylmethanesulfonyl fluoride; SDS−PAGE, sodium dodecyl sulfate−polyacrylamide gel electrophoresis; SLG, *S*-(2-hydroxyacyl)glutathione.

 Published on Web 05/04/2009

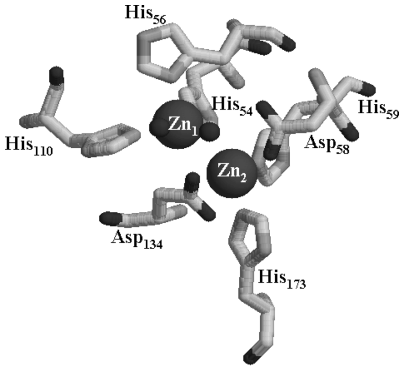

FIGURE 1: Proposed active site of human Glx2 (*40*). The small spheres are solvent molecules, and the large spheres are Zn(II) ions. This figure was rendered using Raswin version 2.7.2.2 (*60*) and Protein Data Bank entry 1qh5.

formation of hyperglycemia-induced advanced glycation end products, suggesting that these enzymes may have a role in diabetic microangiopathy (*30*). Glyoxalase enzymes may also play a role in the pathogenesis of Alzheimer's disease (*31*, *32*). Finally, Glx2 has been identified as a target of p63 and p73 and suggested to be a prosurvival factor of the p53 family of transcription factors (*33*).

Glx2 has been purified and biochemically characterized from many sources, such as plants, mammalian liver, *Salmonella*, and *Escherichia coli* (*34*−*39*). Cameron et al. reported the crystal structure of human Glx2 (*40*), which defined an overall structure and showed the presence of a dinuclear zinc active site similar to those in the enzymes of the metallo-β-lactamase superfamily (*41*, *42*). The structure had two domains: a four-layered α sandwich similar to that seen in metallo-β-lactamases and a predominately α-helical domain (*40*). As with other metallo-β-lactamase family enzymes, the metal ion in the Zn_1 site was coordinated by His54, His56, His110, bridging Asp134, and a bridging hydroxide. The metal ion in the Zn_2 site was coordinated by His59, His173, Asp58, the bridging Asp134, the bridging hydroxide, and a terminally bound solvent molecule (Figure 1). Although the protein used for crystallography contained ~1.5 mol of zinc and 0.7 mol of iron per mole of protein, the authors concluded that human Glx2 contains a dinuclear Zn(II) active site. The issue of iron binding was not considered, but this omission raises questions concerning the actual metal binding preference of human Glx2.

In this paper, we present the results of biochemical and spectroscopic studies of human Glx2. Recombinant human Glx2 was overexpressed in the presence of different combinations of zinc, iron, and cobalt, and the resulting enzymes were then purified to homogeneity. Steady-state kinetic studies were used to determine the catalytic properties of the purified Glx2 analogues. ICP-AES was used to determine the metal content of the purified enzymes, and nuclear magnetic resonance (NMR) and electron paramagnetic resonance spectroscopies (EPR) were used to probe the dinuclear metal centers. These biochemical and spectroscopic results provide detailed structural information about the human Glx2 metal center and insights concerning the structure and kinetic mechanism of the enzyme that may ultimately be used to design inhibitors with potential therapeutic value.

EXPERIMENTAL PROCEDURES

Overexpression and Purification of Human Glx2. PCR was conducted on a plasmid, which contains the gene for Glx2 from *Homo sapiens*, which was kindly provided by B. Mannervik, using the primers CCTCCATGGTAAA-AATCGAACTGGTGC and GAGTCGACTCGAGCTCTA-GATCTTTTTTTTTT that generated *Nde*I and *Hin*dIII restriction sites at the 5′ and 3′ ends of the *glx2* gene. The PCR fragment was subcloned into pET26b using the *Nde*I and *Hin*dIII restriction sites, and the sequence of the resulting pGlx2/pET26b plasmid was confirmed by DNA sequencing. The pGlx2/pET26b plasmid was transformed into *E. coli* BL21(DE3) Rosetta cells, and small scale cultures were used to maximize the recovery of soluble protein at different temperatures (15, 22, 30, and 37 °C). A large-scale overexpression of human Glx2 was performed as follows. A 10 mL overnight culture of *E. coli* BL21(DE3) Rosetta cells containing pGlx2/pET26b was used to inoculate 1 L of LB (Luria-Bertani) medium containing 25 μg/mL kanamycin and 25 μg/mL chloramphenicol. The cells were allowed to grow at 37 °C with shaking until they reached an optical density at 600 nm of 0.6−0.8. Protein production was induced by making the cultures 0.5 mM in isopropyl-β-D-thiogalactopyranoside (IPTG), and the cells were shaken at 22 °C for 24 h. The cells were collected by centrifugation (15 min at 7000*g*), and the cell pellets were stored at −80 °C until further use.

The cell pellet was thawed and resuspended in 15 mL of 10 mM MOPS (pH 6.5) containing 0.1 μM phenylmethanesulfonyl fluoride (PMSF). The cells were French pressed four times at 16000 psi and centrifuged for 30 min at 15000*g* and 4 °C. The supernatant was dialyzed overnight at 4 °C versus 2 L of 10 mM MOPS (pH 6.5). The dialyzed crude protein sample was centrifuged at 15000*g* and was subjected to FPLC using an SP-Sepharose column (1.5 cm × 12 cm with a 25 mL bed volume) that was equilibrated with 10 mM MOPS (pH 6.5). Bound proteins were eluted with a 0 to 500 mM NaCl gradient in 10 mM MOPS (pH 6.5) at a rate of 2 mL/min. Fractions containing human Glx2 were identified by sodium dodecyl sulfate−polyacrylamide gel electrophoresis (SDS−PAGE), pooled, and concentrated by using an Amicon ultrafiltration cell equipped with a YM-10 membrane. Enzyme concentrations were determined by measuring the absorbance at 280 nm and using a molar extinction coefficient of 23080 M^{-1} cm^{-1} (*40*).

Human Glx2 was overexpressed in minimum medium consisting of 2.5 g of glucose, 5 g of casamino acids, 5.5 g of KH_2PO_4, 10.8 g of K_2HPO_4, 1 g of ammonium sulfate, and 10 g of NaCl per 1 L of distilled H_2O in the presence of 100 μM Zn(II), Fe(II), Mn(II), or Co(II) to evaluate its metal binding preference. The resulting enzyme samples were purified as described above.

Metal Analyses. The metal content of Glx2 samples was determined using a Varian-Liberty 150 inductively coupled plasma spectrometer with atomic emission spectroscopy detection (ICP-AES), as described previously (*43*). Protein samples were diluted to 10 μM with 10 mM MOPS (pH 6.5) prior to analysis. A calibration curve with four standards and a correlation coefficient of >0.99 was generated using Fe, Zn(II), Mn, and Co reference solutions. The following emission wavelengths were chosen to ensure the lowest detection limits possible: Fe, 259.940 nm; Zn, 213.856 nm; Mn, 257.610 nm; and Co, 238.892 nm.

To further evaluate metal binding to Glx2, a 3-fold molar excess of $Fe(NH_4)_2(SO_4)_2$, $Zn(SO_4)_2$, or $Fe(NH_4)_2(SO_4)_2$ with $Zn(SO_4)_2$ was added directly to purified as-isolated human Glx2, and the mixtures were allowed to incubate on ice for 1 h. Unbound metal ions were removed by 4 × 1 L dialysis steps

Table 1: Metal Content and Steady-State Kinetic Constants for Human Glx2 Analogues

enzyme	Zn(II) (equiv)	Fe (equiv)	Co or Mn (equiv)	k_{cat} (s^{-1})	K_m (μM)
Glx2-LB	0.4 ± 0.1	0.5 ± 0.1	ND[b] (Mn)	570 ± 99	660 ± 190
Glx2-LB + 1.5Zn + 1.5Fe	1.2 ± 0.1	0.9 ± 0.1	ND[b] (Mn)	740 ± 40	780 ± 68
Glx2-Zn_{min}	1.1 ± 0.2	ND[b]	ND[b] (Mn)	407 ± 13	81 ± 11
Glx2-Zn_{min} + 3equivZn(II)	0.9 ± 0.2	ND[b]	ND[b] (Mn)	262 ± 24	53 ± 22
Glx2-Zn_{min} + 3equivFe(II)	1.0 ± 0.1	0.7 ± 0.1	ND[b] (Mn)	281 ± 28	81 ± 30
Glx2-Zn_{min} in 100 μM Fe buffer	N/A[a]	N/A[a]	N/A[a]	355 ± 24	105 ± 24
Glx2-Zn_{min} in 100 μM Zn(II) buffer	N/A[a]	N/A[a]	N/A[a]	384 ± 9	109 ± 8
Glx2-Fe_{min} + Zn(II)	0.5 ± 0.2	0.6 ± 0.2	ND[b] (Mn)	240 ± 5	256 ± 19
Glx2-Co_{min}	0.1 ± 0.1	0.2 ± 0.1	1.0 ± 0.1 (Co), ND[b] (Mn)	815 ± 36	110 ± 17
Glx2-Co_{min} + 1equivZn(II)	1.0	0.2 ± 0.1	1.0 ± 0.1 Co	565 ± 30	65 ± 13
Glx2-Zn_{min} + 1equivNi	0.1 ± 0.1	0.2 ± 0.1	1.0 Ni	439 ± 6	91 ± 9

[a] Not applicable. [b] None detected.

against 10 mM MOPS (pH 6.5) at 4 °C (12 h for each step). The metal content of these protein samples was determined using ICP-AES as described above.

Steady-State Kinetics. Steady-state kinetic parameters (K_m and k_{cat}) of human Glx2 were determined using *S*-D-lactoylglutathione (SLG) as a substrate. Thioester hydrolysis was monitored at 240 nm over 30 s at 25 °C as previously reported (*43*). The concentration of Glx2 analogues was typically 1−10 nM, and substrate concentrations used were 30−600 μM. The buffer used in the steady-state kinetic studies was 10 mM MOPS (pH 6.5), containing either no added metals, 100 μM $ZnCl_2$, or 100 μM $Fe(NH_4)_2(SO_4)_2$.

Stopped-Flow Kinetic Studies. Stopped-flow UV−vis studies were conducted on an Applied Photophysics SX.18-MVR stopped-flow spectrophotometer at 2 °C. The reaction of Glx2 analogues (final concentration of 32.5 μM) and SLG (final concentration of 60.5 μM) was monitored at 240 nm for 200 ms. Stopped-flow absorbance data were converted to concentration data using the SLG extinction coefficient (−3100 M^{-1} cm^{-1}). All reactions were conducted in triplicate, and reaction rates were determined by fitting the progress curves to a first-order exponential equation.

Spectroscopic Studies. ^{1}H NMR spectra were recorded on a Bruker Avance 500 spectrometer operating at 500.13 MHz and 298 K, with a magnetic field of 11.7 T, a recycle delay (AQ) of 41 ms, and a sweep width of 400 ppm. Chemical shifts were referenced by assigning the H_2O signal a value of 4.70 ppm. A modified presaturation pulse sequence (zgpr) was used to suppress the proton signals originating from solvent and amino acids not coupled to the metal center. Line broadening of 50 Hz was used for all of the spectra. The protein concentration was ~1 mM, and 10% D_2O was included in samples for locking.

EPR spectra were recorded using a Bruker E600 EleXsys spectrometer equipped with an Oxford Instruments ESR900 helium flow cryostat and ITC503 temperature controller, and an ER4116DM cavity operating at 9.63 GHz in perpendicular mode. Other recording parameters are given in the figure legend. Quantitation of Fe(III) signals was conducted by double integration of spectra recorded at nonsaturating power (2 mW) at 12 K. A 2 mM Cu(II)-EDTA standard in HEPES buffer (pH 7.5) recorded at 60 K and 50 μW was used. Integration limits and correction factors for $S = {}^1/_2$ and $S = {}^5/_2$ signals, where *D* is assumed to be small compared to temperature, were employed (*44*−*46*). Co(II) signals were quantified by double integration, with reference to a frozen aqueous reference sample containing 2 mM Co(II), 50 mM imidazole, and 10% by volume glycerol, recorded at 12 K and 0.8 mW. EPR simulations were performed using XSophe (Bruker Biospin), assuming $S = {}^3/_2$ and $|D| \gg h\nu$.

RESULTS

Overexpression and Purification of Human Glx2. High levels of soluble human Glx2 were produced in *E. coli* BL21(DE3) Rosetta cells grown in LB medium at 22 °C. The colorless recombinant protein eluted via SP-Sepharose chromatography at 100 mM NaCl in 10 mM MOPS (pH 6.5). Approximately 20 mg of purified Glx2 per liter of culture was obtained using this method. Human Glx2, overexpressed in LB medium (Glx2-LB), was shown to bind 0.4 ± 0.1 equiv of Zn(II) and 0.5 ± 0.1 equiv of Fe (Table 1). After incubation with 1.5 equiv of Zn(II) and 1.5 equiv of Fe(II), followed by exhaustive dialysis, human Glx2 (Glx2-LB + 1.5Zn + 1.5Fe) was shown to bind 1.2 ± 0.1 equiv of Zn(II) and 0.9 ± 0.1 equiv of Fe (Table 1).

Metal Binding to Human Glx2. Metal binding to human Glx2 was further evaluated by expressing the enzyme in minimum medium containing various metal ions, and the metal content of the resulting enzymes was analyzed by ICP-AES (Table 1). Glx2, overexpressed in the presence of 100 μM $ZnCl_2$ (Glx2-Zn_{min}), bound 1.1 ± 0.2 equiv of Zn(II) and < 0.005 equiv of Fe or Mn. When 3 equiv of Zn(II) was added to this enzyme, followed by exhaustive dialysis, the resulting enzyme [Glx2-Zn_{min} + 3equivZn(II)] was shown to bind 0.9 ± 0.2 equiv of Zn(II) and < 0.005 equiv of Fe or Mn. When 3 equiv of Fe(II) was added to Glx2-Zn_{min} followed by dialysis, the resulting enzyme [Glx2-Zn_{min} + 3equivFe(II)] was shown to bind 1.0 ± 0.1 equiv of Zn(II) and 0.7 ± 0.1 equiv of Fe.

Overexpression of human Glx2 in minimum medium containing 100 μM $Fe(NH_4)_2(SO_4)_2$ or 100 μM $MnCl_2$ did not result in appreciable amounts of enzyme at any temperature. However, when 5 μM $ZnCl_2$ was added to the minimal medium containing Fe(II), human Glx2 was overexpressed, and the purified enzyme [Glx2-Fe_{min} + Zn(II) in Table 1] was found to contain 0.5 ± 0.2 equiv of Zn(II) and 0.6 ± 0.2 equiv of Fe. This result suggests that human Glx2 needs Zn(II) to be overexpressed and that the enzyme may bind 1 mol each of iron and zinc per mole of enzyme. We tested this hypothesis by incubating Glx2-LB with 1.5 equiv of Zn(II) and Fe(II), and the resulting enzyme (Glx2-LB + 1.5Zn + 1.5Fe) was exhaustively dialyzed. Consistent with our hypothesis, Glx2-LB + 1.5Zn + 1.5Fe was shown to bind 1.2 ± 0.1 equiv of Zn(II) and 0.9 ± 0.1 equiv of Fe.

Since none of the human Glx2 samples contained significant amount of Mn, we did not determine the effect of adding Zn(II) to minimal medium containing Mn(II) on Glx2 overexpression.

We did, however, find that human GLX2 does bind cobalt. When the enzyme was overexpressed in minimal medium containing 100 μM $CoCl_2$, Glx2-Co_{min} bound 0.1 ± 0.1 equiv of Zn(II), 0.2 ± 0.1 equiv of Fe, and 1.0 ± 0.1 equiv of Co. Therefore, human Glx2 preferentially binds 1 mol each of Fe and Zn(II) per mole of enzyme and can bind 1 mol of Co, but it does not bind Mn.

Steady-State Kinetics. Steady-state kinetic studies were performed on the different forms of human Glx2 to evaluate the effect of different metal ions on the catalytic activity of the enzyme. Glx2-LB, which contained 0.4 ± 0.1 equiv of Zn(II) and 0.5 ± 0.1 equiv of Fe, exhibited a k_{cat} of 570 ± 99 s^{-1} and a K_m of 660 ± 190 μM (Table 1). Interestingly, Glx2-LB + 1.5Zn + 1.5Fe, which contained 1.2 ± 0.1 equiv of Zn(II) and 0.9 ± 0.1 equiv of Fe, exhibited relatively similar values [k_{cat} of 740 ± 40 s^{-1} and K_m of 780 ± 68 μM (Table 1)]. Glx2-Zn_{min} exhibited a k_{cat} of 407 ± 13 s^{-1} and a K_m of 81 ± 11 μM, while purified Glx2-Zn_{min}, which was incubated with 3 equiv or Zn(II) or Fe(II) to increase the Zn(II) or Fe(II) content, respectively, exhibited k_{cat} values of 262 ± 24 and 281 ± 28 s^{-1} and K_m values of 53 ± 22 and 81 ± 30 μM, respectively. Inclusion of 100 μM Fe(II) or Zn(II) in the assay buffer for Glx2-Zn_{min} in an attempt to further load the enzyme with metal did not significantly affect the kinetic constants (Table 1). These results suggest that human Glx2 requires only 1 equiv of Zn(II) for activity. However, Glx2-Co_{min} was also shown to be active with SLG (k_{cat} of 815 ± 36 s^{-1} and K_m of 110 ± 17 μM). The direct addition of 1 equiv of Co(II) to Glx2-Zn_{min} or Glx2-Co_{min} resulted in the formation of a yellow precipitate, most likely due to oxidation of Co(II) to Co(III).

Stopped-Flow Kinetic Studies. To further probe the kinetic behavior of the different human Glx2 analogues, stopped-flow kinetic studies were conducted in which the disappearance of substrate SLG was monitored over time (Figure 2). Each reaction mixture contained 33 μM SLG and 60 μM Glx2 analogue. Glx2-LB, which contained 0.4 equiv of Zn(II) and 0.5 equiv of Fe, exhibited a rate of 30 ± 1 s^{-1}. Glx2-Zn_{min}, Glx2-Zn_{min} + 3equivFe(II), Glx2-Zn_{min} + 3equivZn(II), and Glx2-LB + 1.5Zn + 1.5Fe analogues exhibited essentially the same rate of 49 ± 3 s^{-1}. The Glx2-Fe_{min} + Zn(II) analogue, which contains 0.5 and 0.6 equiv of Zn(II) and Fe, respectively, exhibited the slowest rate (15 ± 1 s^{-1}). On the other hand, Glx2-Co_{min}, which contains 0.1 equiv of Zn(II), 0.2 equiv of Fe, and 1.0 equiv of Co, exhibited the fastest rate (139 ± 2 s^{-1}).

Spectroscopic Studies. ^{1}H NMR spectroscopy was utilized to probe the metal binding sites of human Glx2. A ^{1}H NMR spectrum of Glx2 containing 1.2 ± 0.1 equiv of Zn(II) and 0.9 ± 0.1 equiv of Fe (Glx2-LB + 1.5Zn + 1.5Fe) showed two solvent-exchangeable peaks at 47 and 71 ppm (Figure 3A). Given the line widths of these signals and the fact that the predicted Zn_2 site has two histidines while the Zn_1 site has three histidines (*40*), we predict that there is a Fe(II) bound to the Zn_2 site in this sample. Nonetheless, we cannot completely discount the possibility that Fe(II) is binding to a histidine from each site or the possibility that Fe(II) is binding to the Zn_1 site and one of the histidine NH protons is in fast exchange with solvent.

The ^{1}H NMR spectrum of Glx2 containing 1.0 ± 0.1 equiv of Co(II) (Table 1) exhibited five paramagnetically shifted resonances (Figure 3B). The peaks at 55, 71, and 87 ppm completely disappear, and the peak at 42 ppm decreased by helf when the sample was exchanged in 90% D_2O. This result indicates that there are at least four solvent-exchangeable peaks in the Glx2-Co_{min} sample. The peak at 87 ppm (spectrum B in Figure 3) is larger than the other peaks, suggesting that this peak may be due

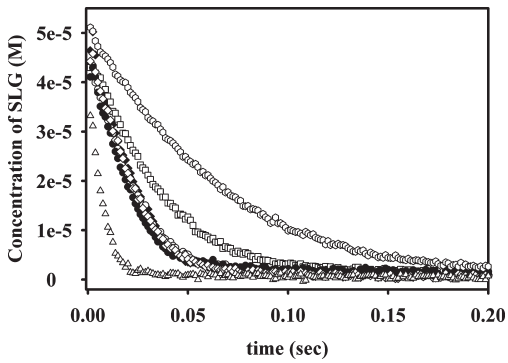

FIGURE 2: Stopped-flow kinetic studies of the reaction of human Glx2 analogues with SLG at 2 °C. The concentration of Glx2 analogues was 32.5 μM, and the concentration for SLG was 60.5 μM. The following progress curves are shown: (⬡) Glx2-Fe_{min} + Zn(II), (□) Glx2-LB, (●) Glx2-Zn_{min}, (◆) Glx2-Zn_{min} + 3equivZn(II), (◇) Glx2-Zn_{min} + 3equivFe(II), (○) Glx2-LB + 1.5Zn + 1.5Fe, and (△) Glx2-Co_{min}. The progress curves for Glx2-Zn_{min}, Glx2-Zn_{min} + 3equivZn(II), Glx2-Zn_{min} + 3equivFe(II), and Glx2-LB + 1.5Zn + 1.5Fe were nearly superimposable.

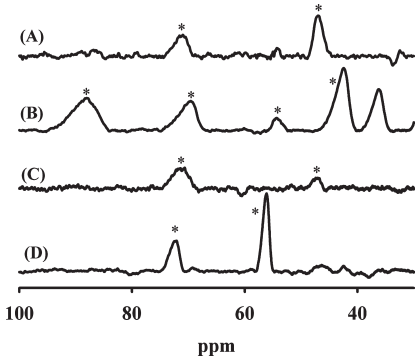

FIGURE 3: ^{1}H NMR spectra of human Glx2 analogues in 10 mM MOPS (pH 6.5) containing 10% D_2O: (A) Glx2-LB + 1.5Zn + 1.5Fe, (B) Glx2-Co_{min}, (C) Glx2-Co_{min} with 1 equiv of Zn(II) added, and (D) ZnNi-Glx2. The enzyme concentrations in these samples were ~1 mM. The asterisks denote peaks that were solvent-exchangeable. The magnitude of the peak at 42 ppm in the spectrum of Glx2-Co_{min} decreased by half when the sample was exchanged in 90% D_2O.

to two protons both of which are solvent-exchangeable. The NMR spectrum of Glx2-Co_{min} suggests that Co(II) binds to four or five histidines and, therefore, that Co(II) binds to both the Zn_1 and Zn_2 sites in human Glx2.

To probe whether Zn(II) could displace Co(II) from one of the metal binding sites, 1 equiv of Zn(II) was added to Glx2-Co_{min} to generate Glx2-Co_{min} + 1equivZn(II). The resulting analogue exhibited a k_{cat} of 565 ± 30 s^{-1} and a K_m of 65 ± 13 μM, when using SLG as the substrate (Table 1). The NMR spectrum of this analogue exhibited two solvent-exchangeable peaks at 47 and 71 ppm (Figure 3C), which are the same positions as the solvent-exchangeable peaks for the Glx2-LB + 1.5Zn + 1.5Fe sample (Figure 3A). This result suggests that Glx2 preferentially binds Zn(II) over Co(II) in the Zn_1 site, but not in the Zn_2 site.

To test whether the Zn_2 site can bind other metal ions in addition to Co(II) and Fe(II), we added 1 equiv of Ni(II) to Glx2-Zn_{min} to generate a ZnNi analogue of human Glx2. Glx2-Zn_{min} with 1 equiv of Ni exhibited a k_{cat} of 439 ± 6 s^{-1} and a K_m of 91 ± 9 μM when using SLG as the substrate (Table 1). A ^{1}H NMR spectrum of ZnNi-Glx2 showed two relatively sharp, solvent-exchangeable peaks at 57 and 73 ppm (Figure 3D). In agreement with the other NMR studies, this result suggests that Ni(II) exhibits a preference for binding to the consensus Zn_2 site.

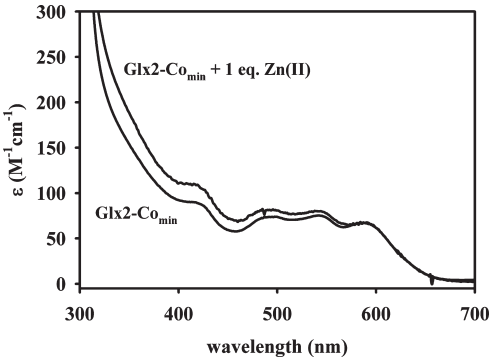

FIGURE 4: UV−vis spectra of Glx2-Co_{min} and Glx2-Co_{min} + 1equivZn(II). The buffer in these samples was 10 mM MOPS (pH 6.5), and the enzyme concentration was 1.6 mM.

UV−vis spectra of Co(II)-containing Glx2 samples were recorded in an effort to obtain information about the coordination number of Co(II) in these samples (Figure 4). The spectrum of Glx2-Co_{min} exhibited three peaks between 500 and 600 nm, which we assign to ligand field transitions of high-spin Co(II) and a weaker feature at 410 nm, which we assign to the presence of Co(III) (*47*). The extinction coefficient of the ligand field transitions ranged from 28 to 42 M^{-1} cm^{-1}, which suggests that the Co(II)'s are five- or six-coordinate. The addition of 1 equiv of Zn(II) to the Glx2-Co_{min} sample did not result in a change in the intensities of the ligand field transitions or the feature assigned to Co(III). This result suggests that both Co(II)'s in Glx2-Co_{min} are five- or six-coordinate. There was an increase in the magnitude of the 280 nm peak, which resulted in a relatively higher absorption of the feature at 410 nm, and a slightly higher absorbance of the ligand field transitions at 500 and 550 nm was due to enzyme precipitation when Zn(II) was added to the sample.

Essentially indistinguishable EPR spectra were observed for both Glx2-LB and Glx2-LB + 1.5Zn + 1.5Fe and were dominated by a g_{eff} = 4.3 signal due to Fe(III) (Figure 5). Unlike the rich spectra observed from other Glx2 species, such as *Arabidopsis* mitochondrial Glx2−5 (*34*, *48*, *49*), the $S = {}^5/_2$ signals from human Glx2 contained no well-resolved features other than the g_{eff} = 4.3 line. This result suggests very high strains in the rhombic zero-field splitting term, E/D, and provides no confirmatory evidence of binding of Fe(III) to human Glx2 in a well-defined tight binding site. The intensities of the spectra from human Glx2 were equivalent and accounted for ≤0.2 Fe(III) per Glx2 molecule, suggesting that the majority of iron in the samples was present as Fe(II). A small feature at 3600 G (360 mT) suggested the possibility of an Fe(III)Fe(II) center, as in Glx2−5 (*34*), in a small proportion of the molecules (Figure 3C). This was the only evidence for bona fide binding of Fe(III) to Glx2. The spectrum also revealed a complex pattern of lines in the g_{eff} = 2 region that, from comparison with a standard Mn(II) signal, suggested trace amounts of Mn(II), likely adventitiously bound.

EPR spectra of Glx2-Co_{min} indicated that only ∼25% of the Co(II) in Glx2 was EPR-visible. The EPR spectrum itself, recorded under nonsaturating conditions, was complex (Figure 6A). Individual species were deconvoluted by preferential saturation of spectral components and by the collection and analysis of spectra recorded under rapid passage conditions, in the presence of three distinct Co(II) species. The EPR spectrum recorded under partially saturating conditions (Figure 6B) indicated that the derivative feature at 2040 G is not associated with either the large absorption-shaped component at 1110 G or the

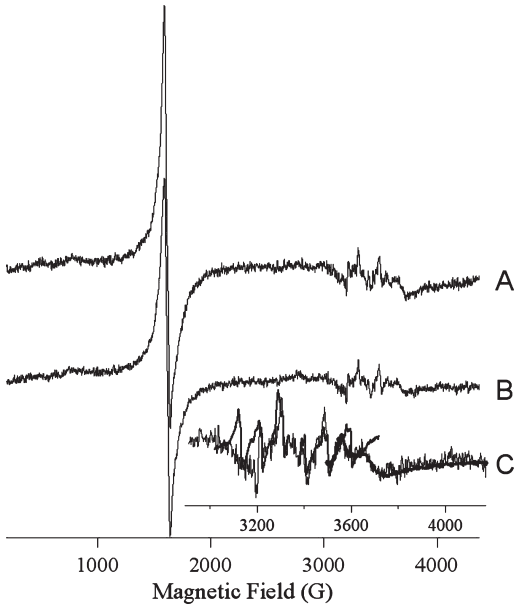

FIGURE 5: EPR spectra of human Glx2 analogues (A) Glx2-LB and (B) Glx2-LB + 1.5Zn + 1.5 Fe. Trace C shows the $g \sim 2$ region of trace B expanded (thin line). Overlaid are a spectrum of Mn(II) in modeling wax (thick line) and a signal from an Fe(III)Fe(II) center in Glx2−1 from *Arabidopsis thaliana* (thick line with circular markers). A signal due to Cu(II) in the spectrometer cavity was subtracted from the experimental traces of human glyoxylase, and imperfect subtraction is likely responsible for the poor correlation of the Mn(II) reference signal with the glyoxylase signal in the $g \sim 2.01$ region [3100−3200 G; this is where the intense $g_{\perp}$ feature of Cu(II) is observed]. Spectra were recorded at a microwave power of 2 mW, 10 K, and a magnetic field modulation of 12 G (1.2 mT) at 100 kHz.

derivative feature at 2660 G. Comparison of two rapid-passage spectra recorded at different microwave powers (Figure 6C,D) indicated that the derivative feature at 2660 G was associated with the broad absorption "tail" centered around 4000 G, and likely with some absorption in the 800−1600 G range. Subtraction of appropriate amounts of Figure 6D from Figure 6C yielded an apparently single-component axial signal that was readily simulated as an $M_S = \pm{}^1/_2$ species with an E/D of 0.1. The experimental data, therefore, clearly identified that three distinct species contributed to the spectrum and provided a full set of parameters for one of them. Using the axial species, the two associated features at 2660 and 4000 G from Figure 6D, and the distinct feature at 2040 G from Figure 6B as a basis for three species, the experimental spectrum recorded under nonsaturating conditions was best simulated using the parameters described in the legend of Figure 6. The simulations indicate that two of the species are likely five-coordinate and the third is either five- or six-coordinate. It is of note that for one of the species, that of Figure 6B, the g_{real} values are unusually high for Co(II) in a metalloprotein, though not excessively so. Our assignment to $M_S = \pm{}^1/_2$, and five-coordinate geometry, is based on comparison of the resultant g_{real} values of 2.9, 2.9, and 3.0 with those returned by assuming the alternative $M_S = \pm{}^3/_2$ manifold, and hence distorted tetrahedral geometry, of 3.4, 3.4, and 3.0, respectively. These latter values would be unprecedented for Co(II) in an environment of the types found in the Glx2 active site.

DISCUSSION

The metallo-β-lactamase fold consists of an $\alpha\beta/\beta\alpha$ sandwich motif, made up of a core unit of two β-sheets surrounded by solvent-exposed helices (*41*, *42*). Members of this superfamily

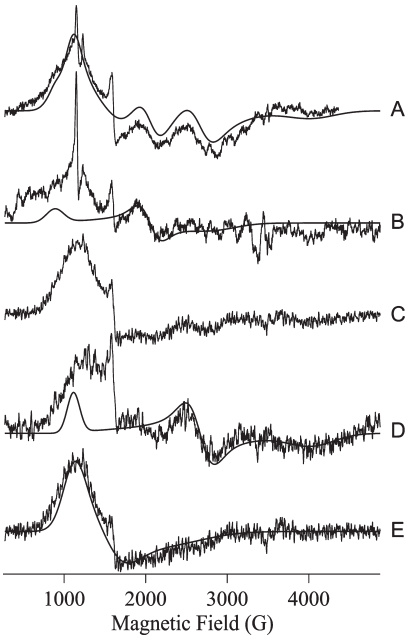

FIGURE 6: EPR spectra of human Glx2 containing Co(II). (A) Experimental EPR spectrum of 1.7 mM Glx2 incubated with 1.7 mM Co(II), recorded at 12 K and 0.8 mW. The doubly integrated intensity of the spectrum corresponded to 0.4 mM Co(II). A simulated spectrum is overlaid; the simulated spectrum was generated by adding 0.21, 0.44, and 0.35 fractional spin equivalent of computed spectra B, D, and E, respectively. (B), Experimental spectrum recorded at 7.6 K and 100 mW and a computed spectrum with the following spin Hamiltonian parameters: $S = {}^3/_2$, $M_S = {}^1/_2$ ($E \gg g\beta SH$), $g_\parallel = 3.0$, $g_\perp = 2.9$, and $E/D = 0.28$. (C) Rapid-passage $\delta\chi''/\delta H$ EPR spectrum recorded at 7.6 K and 100 mW. The experimental pseudoabsorption spectrum was collected with second-harmonic out-of-phase modulation-phase-sensitive detection. The derivative spectrum shown was generated by differentiating the experimental spectrum, applying 20 G pseudomodulation. (D) Rapid-passage $\delta\chi''/\delta H$ EPR spectrum recorded at 7.6 K and 10 mW. A computed spectrum is overlaid, with the following parameters: $S = {}^3/_2$, $M_S = {}^1/_2$ ($E \gg g\beta SH$), $g_\parallel = 2.15$, $g_\perp = 2.3$, and $E/D = 0.29$. (E) Difference spectrum generated by subtraction of a fraction of the experimental spectrum D from spectrum C and an overlaid computed spectrum with the following parameters: $S = {}^3/_2$, $M_S = {}^1/_2$ ($E \gg g\beta SH$), $g_\parallel = 2.9$, $g_\perp = 2.6$, and $E/D = 0.10$. All spectra were recorded with a magnetic field modulation of 12 G at 100 kHz.

contain a conserved HXHXD motif that has been shown to bind Zn(II), Fe, and Mn. There are several enzymes in the metallo-β-lactamase fold family, including metallo-β-lactamases, glyoxalase II, lactonase, rubredoxin:oxygen oxidoreductase (ROO), arylsulfatase, phosphodiesterase, and tRNA maturase (*50*). Most of the members of the metallo-β-lactamase superfamily (metallo-β-lactamases, tRNA maturase, phosphodiesterase, arylsulfatase, and lactonase) appear to contain dinuclear Zn(II) centers. On the other hand, rubredoxin:oxygen oxidoreductase (ROO) appears to contain a dinuclear iron center (*51*). Glx2 from *E. coli* was recently reported to contain a dinuclear Zn(II) center (*35*), while plant mitochondrial Glx2 (Glx2−5) has been shown to contain a FeZn center (*34*). Interestingly, plant cytoplasmic Glx2 (*48*, *49*) and Glx2 from *Salmonella typhimurium* (*39*) can exist with a number of possible metal centers, including dinuclear Fe, FeZn, MnZn, and presumably dinuclear Zn(II). On the basis of a crystal structure, human Glx2 was reported to contain a dinuclear Zn(II) center, although the enzyme used for the crystallization studies contained 1.5 equiv of Zn(II) and 0.7 equiv of Fe (*40*).

To more clearly define the metal binding properties of human Glx2, the protein was overexpressed in either LB or minimum medium containing different metal ions. Human Glx2 overexpressed in LB medium bound roughly equal, albeit substoichiometric, amounts of Zn(II) and Fe and exhibited a k_{cat} of 570 s^{-1} and a very large K_m value of 660 μM (Table 1). Addition of Zn(II) and Fe to this enzyme followed by dialysis resulted in an enzyme (Glx2-LB + 1.5Zn + 1.5Fe) that bound 1.2 ± 0.1 equiv of Zn(II) and 0.9 ± 0.1 equiv of Fe and exhibited an ~20% higher k_{cat} and a similar K_m (within error) value. The similar K_m values suggest a common active species, yet a 2-fold increase in metal content did not correspond to a 2-fold increase in k_{cat}. This result is most likely due to the as yet unexplained drop in activity when Glx2 samples are dialyzed (*43*, *52*). There were also drops in k_{cat} when Glx2-Zn_{min} was incubated with Zn(II) or Fe, followed by dialysis (Table 1).

The large K_m values exhibited by human Glx2 samples prepared from LB medium were not observed for any of the Glx2 analogues prepared from minimal medium (Table 1). This result suggests that the samples prepared in LB contain a competitive inhibitor, perhaps a peptide from the LB medium. The presence of a competitive inhibitor in the enzymes cultured in LB is supported by the stopped-flow studies that exhibit a lower activity for Glx2-LB [less Zn(II)] and a similar activity for Glx2-LB + 1.5Zn + 1.5Fe analogues as compared to the Glx2 samples prepared in minimal medium (Figure 2). The ^{1}H NMR spectrum of Glx2-LB + 1.5Zn + 1.5Fe did not reveal any unassigned peaks (Figure 3), suggesting that a peptide does not bind directly to the Fe(II) center. However, it is possible that resonances from protons on a metal-bound peptide may not shift to downfield positions greater than 30 ppm. In addition, the crystal structure of human Glx2 identified a number of active site residues that interact with groups on glutathione (*40*), so the binding of a peptide to the metal may not be required for a Glx2−peptide complex to form. MALDI-TOF mass spectrometry was used to compare multiple Glx2 samples prepared in LB and minimal medium in an effort to identify a bound competitive inhibitor; however, no differences in the masses of the different GLX2 analogues were identified. It is possible that the ionization process coupled with the acidic matrix used in the MALDI technique resulted in the loss of the inhibitor.

In an effort to obtain human Glx2 containing only one metal ion, the enzyme was overexpressed in minimal medium containing either Zn(II) or Fe(II). Glx2 overexpressed in minimal medium containing Zn(II) (Glx2-Zn_{min}) was shown to bind 1.1 ± 0.2 equiv of Zn(II) and no detectable Fe or Mn (Table 1). When Glx2-Zn_{min} was incubated with a 3-fold excess of Zn(II) and unbound Zn(II) was removed by dialysis, the resulting enzyme contained 0.9 ± 0.2 equiv of Zn(II). It is unlikely that the samples of Glx2-Zn_{min} contain a mixture of ZnZn-Glx2 and apo-Glx2, since we are unable to prepare an analogue of Glx2 containing 2 equiv of Zn(II) by adding Zn(II) to the sample. This result is in contrast to the crystallographic conclusion that human Glx2 contains a dinuclear Zn(II) metal center (*40*). With regard to iron in Glx2, both NMR and EPR indicated that iron in the iron-containing forms of Glx2 was largely in the Fe(II) state. However, sufficient iron (≈ 20%) was present as Fe(III) to provide for an easily observed EPR signal. Almost all of the Fe(III), however, was present as mononuclear Fe(III), and only a very small signal that was suggestive of an Fe(III)Fe(II) center was observed. These data argue against any significant proportion of di-iron Glx2. On the other hand, human Glx2 can bind two metal ions, and metal analyses and spectroscopic studies suggest that Zn(II) binds in the consensus Zn_1 site, while Ni(II), Co(II), and Fe(II)

can bind in the consensus Zn_2 site. The formation of mixed-metal analogues is not surprising since mixed-metal analogues of several metallo-β-lactamases have been reported (*53*−*55*). However, a surprising result is that a CoCo analogue of human Glx2 can be prepared (Figure 3), while the biophysically and biochemically similar dinuclear Zn(II) analogue cannot be prepared (see metal analysis data above). Given the bioavailability of the metal ions tested (*56*), we hypothesize that human Glx2 contains a Zn(II)Fe(II) center in vivo. Unlike *Arabidopsis* Glx2−2 (*49*, *57*), dinuclear Fe- or Zn(II)-containing analogues of human Glx2 cannot be prepared.

The steady-state kinetic studies on Glx2 samples prepared in minimal medium revealed some surprising results with respect to metal content and activity. Glx2-Zn_{min}, which contains ~1 equiv of Zn(II), is the most active Zn(II)-containing form of these analogues (Table 1), and the presence of Zn(II) or Fe(II) in the assay buffer does not greatly affect the activity of the enzyme. This result demonstrates that a dinuclear metal center is not required for the full catalytic activity of human Glx2 and that the second metal ion does not play a large role in catalysis. The steady-state kinetic data did reveal that Glx2-Zn_{min}, which was incubated with 3 equiv of Zn(II) or Fe(II), exhibited similar albeit lower activities. This lower activity is probably due to the dilute (low nanomolar) enzyme being somewhat unstable after dialysis. At the higher concentrations used in the stopped-flow studies, the Glx2-Zn_{min} + Zn and Glx2-Zn_{min} + Fe analogues exhibited rates similar to that of Glx2-Zn_{min} (Figure 2). The steady-state and stopped-flow kinetic data for the Glx2-Zn_{min} samples after incubation with Zn(II) or Fe(II) and dialysis show that Fe has little or no effect on the activity of the enzyme. These data clearly show that human Glx2 is active when there is a mononuclear Zn(II) bound to the enzyme, presumably in the Zn_1 site. This result is important for the rational design of inhibitors that target the metal binding site.

The most active form of human Glx2 is Glx2-Co_{min} (Table 1 and Figure 2). NMR studies show that Co(II) binds to both metal binding sites in this analogue (Figure 3). EPR spectra of Glx2-Co_{min} revealed the presence of three distinct Co(II) species, two rhombic and one axial. The exhibition of both an axial and a rhombic signal from a single Co(II) binding site has been observed in a number of instances and, in some cases, has been shown to be due to the different effects of water and hydroxyl ligands, in a pH-dependent equilibrium, on EPR strain parameters (*58*). However, the presence of two highly rhombic species, and three species overall, indicates at least two Co(II) binding sites, and the spin Hamiltonian parameters indicate five- or six-fold coordination in each case. These data are entirely in accord with the NMR results, showing binding to both Zn_1 and Zn_2 sites, and with the five- or six-fold coordination indicated by the electronic absorption spectrum. The Co(II) EPR signals accounted for only ~25% of the total Co(II) and corresponded to a population of Glx2 in which either the Zn_1 or Zn_2 site was occupied. Most of the Co(II) in Glx2, then, is likely present in a dinuclear site that is EPR-silent due to antiferromagnetic coupling. This coupling need only be very weak, on the order of a wavenumber, to preclude observation of an EPR signal. When 1 equiv of Zn(II) is added to this enzyme, Zn(II) presumably displaces Co(II) from the Zn_1 site, and the resulting ZnCo analogue exhibits activity similar to that of Glx2-Zn_{min}. These results suggest that the most active analogue of human Glx2 has Co(II) in the Zn_1 site and that the metal ion in the Zn_2 site plays little role in catalysis. We have attempted to prepare a CoCo analogue of human Glx2 by adding Co(II) to Glx2-Co_{min}; however, the enzyme precipitates upon addition of Co(II). It is not clear why Glx2-Co_{min} is more active than the corresponding Glx2-Zn_{min} or ZnCo analogues; however, the greater Lewis acidity of Co(II) as compared to that of Zn(II) may explain some of the differences (*59*). Co(II)-substituted liver alcohol dehydrogenase is 140% more active than the corresponding Zn(II)-containing enzyme (*59*). In spite of greater activity, the relatively lower bioavailability of Co(II), as compared to that of Zn(II) or Fe, strongly suggests that human Glx2 is not a Co(II)-containing enzyme.

The results present here demonstrate that human Glx2 is active as a mononuclear Zn(II)-containing enzyme and that Zn(II) binds preferentially to the consensus Zn_1 site. This finding is similar to a recent study that reported that metallo-β-lactamase L1 is active as a mononuclear Zn(II) enzyme when Zn(II) is bound in the Zn_1 site (*53*). The metal content of the active forms of other enzymes belonging to the metallo-β-lactamase superfamily is not clear. Unlike the other enzymes in this superfamily, the metal ion in the Zn_2 site does not appear to play a significant role in human Glx2. Nonetheless, given the bioavailability of Zn(II) and Fe in cells (*56*), we predict that human Glx2 contains a Zn(II)Fe(II) metal binding site in vivo and not a Zn(II)Zn(II) site as previously reported (*40*).

It has been proposed that the enzymes in the metallo-β-lactamase superfamily arose due to a gene duplication event (*50*), and the presence of a dinuclear metal binding site may offer some of the enzymes increased activity. Since Glx2 appears to be a critical enzyme involved in the cellular detoxification of 2-oxoaldehydes (*1*), it may have evolved to be active with only one metal ion, so that the enzyme is active in the presence of low Zn(II) concentrations. The ability to utilize only the single, non-redox active Zn(II) site for catalysis would better position the enzyme to react with the oxidizing substrates.

REFERENCES

1. Mannervik, B. (2008) Molecular enzymology of the glyoxalase system. *Drug Metab. Drug Interact. 23*, 13–27.
2. Thornalley, P. (1993) The glyoxalase system in health and disease. *Mol. Aspects Med. 14*, 287–371.
3. Thornalley, P. J. (1990) The glyoxalase system: New developments towards functional characterization of a metabolic pathway fundamental to biological life. *Biochem. J. 269*, 1–11.
4. Vander Jagt, D. L., and Hunsaker, L. A. (2003) Methylglyoxal metabolism and diabetic complications: Roles of aldose reductase, glyoxalase-1, betaine aldehyde dehydrogenase and 2-oxoaldehyde dehydrogenase. *Chem.-Biol. Interact. 143*, 341–351.
5. Thornalley, P. (1995) Advances in glyoxalase research. Glyoxalase expression in malignancy, anti-proliferative effects of methylglyoxal, glyoxalase I inhibitor diesters, and S-D-lactoylglutathione, and methylglyoxal-modified protein binding and endocytosis by the advanced glycation endproduct receptor. *Crit. Rev. Oncol. Hematol. 20*, 99–128.
6. Thornalley, P. J. (1994) Methylglyoxal, glyoxalases and the development of diabetic complications. *Amino Acids 6*, 15–23.
7. Vander Jagt, D. L. (1993) Glyoxalase II: Molecular characteristics, kinetics, and mechanism. *Biochem. Soc. Trans. 21*, 522–527.
8. Sukdeo, N., and Honek, J. F. (2008) Microbial glyoxalase enzymes: Metalloenzymes controlling cellular levels of methylglyoxal. *Drug Metab. Drug Interact. 23*, 29–50.
9. Yang, K. W., Sobieski, D. N., Carenbauer, A. L., Crawford, P. A., Makaroff, C. A., and Crowder, M. W. (2003) Explaining the inhibition of glyoxalase II by 9-fluorenylmethoxycarbonyl-protected glutathione derivative. *Arch. Biochem. Biophys. 414*, 271–278.
10. Kalsi, A., Kavarana, M. J., Lu, T. F., Whalen, D. L., Hamilton, D. S., and Creighton, D. J. (2000) Role of hydrophobic interactions in binding S-(N-aryl/alkyl-N-hydroxycarbamoyl)glutathiones to the active site of the antitumor target enzyme glyoxalase I. *J. Med. Chem. 43*, 3981–3986.

11. Tew, K. D. (2000) Is there a role for glyoxalase I inhibitors as antitumor drugs?. *Drug Resist. Updates 3*, 263–264.
12. Vince, R., Brownwell, J., and Akella, L. B. (1999) Synthesis and activity of γ-(L-γ-azaglutamyl)-S-(*p*-bromobenzyl)-L-cysteinylglycine: A metabolically stable inhibitor of glyoxalase I. *Bioorg. Med. Chem. Lett. 9*, 853–856.
13. Kavarana, M. J., Kovaleva, E. G., Creighton, D. J., Wollman, M. B., and Eiseman, J. L. (1999) Mechanism-based competitive inhibitors of glyoxalase I: Intracellular delivery, *in vitro* antitumor activities, and stabilities in human serum and mouse serum. *J. Med. Chem. 42*, 221–228.
14. Elia, A. C., Chyan, M. K., Principato, G. B., Giovannini, E., Rosi, G., and Norton, S. J. (1995) N,S-Bis-fluorenylmethoxycarbonylglutathione: A new, very potent inhibitor of mammalian glyoxalase II. *Biochem. Mol. Biol. Int. 35*, 763–771.
15. Thornalley, P. J., Strath, M., and Wilson, R. J. H. (1994) Antimalarial activity *in vitro* of the glyoxalase-I inhibitor diester, S-*p*-bromobenzylglutathione diethyl ester. *Biochem. Pharmacol. 47*, 418–420.
16. Chyan, M. K., Elia, A. C., Principato, G. B., Giovannini, E., Rosi, G., and Norton, S. J. (1995) S-Fluorenylmethoxycarbonyl glutathione and diesters: Inhibition of mammalian glyoxalase II. *Enzyme Protein 48*, 164–173.
17. Murthy, N. S. R. K., Bakeris, T., Kavarana, M. J., Hamilton, D. S., Lan, Y., and Creighton, D. J. (1994) S-(N-Aryl-N-hydroxycarbamoyl)glutathione derivatives are tight-binding inhibitors of glyoxalase I and slow substrates for glyoxalase II. *J. Med. Chem. 37*, 2161–2166.
18. Norton, S. J., Elia, A. C., Chyan, M. K., Gillis, G., Frenzel, C., and Principato, G. B. (1993) Inhibitors and inhibition studies of mammalian glyoxalase II activity. *Biochem. Soc. Trans. 21*, 545–548.
19. Chyan, M. K., Elia, A. C., Principato, G. B., Giovannini, E., Rosi, G., and Norton, S. J. (1994) S-Fluorenylmethoxycarbonyl glutathione and diesters: Inhibition of mammalian glyoxalase-II. *Enzyme Protein 48*, 164–173.
20. Thornalley, P. J. (1993) Modification of the glyoxalase system in disease processes and prospects for therapeutic strategies. *Biochem. Soc. Trans. 21*, 531–534.
21. Edwards, L., Adesida, A., and Thornalley, P. (1996) Inhibition of human leukaemia 60 cell growth by S-D-lactoylglutathione *in vitro*. Mediation by metabolism to N-D-lactoylcysteine and induction of apoptosis. *Leuk. Res. 20*, 17–26.
22. Ratliff, D. M., Vander Jagt, D. J., Eaton, R. P., and Vander Jagt, D. L. (1996) Increased levels of methylglyoxal-metabolizing enzymes in mononuclear and polymorphonuclear cells from insulin-dependent diabetic patients with diabetic complications: Aldose reductase, glyoxalase I, and glyoxalase II—A clinical research center study. *J. Clin. Endocrinol. Metab. 81*, 488–492.
23. Sharkey, E. M., O'Neill, H. B., Kavarana, M. J., Wang, H. B., Creighton, D. J., Sentz, D. L., and Eiseman, J. L. (2000) Pharmacokinetics and antitumor properties in tumor-bearing mice of an enediol analogue inhibitor of glyoxalase I. *Cancer Chemother. Pharmacol. 46*, 156–166.
24. Rulli, A., Carli, L., Romani, R., Baroni, T., Giovannini, E., Rosi, G., and Talesa, V. (2001) Expression of glyoxalase I and II in normal and breast cancer tissues. *Breast Cancer Res. Treat. 66*, 67–72.
25. Antognelli, C., Baldracchini, F., Talesa, V. N., Costantini, E., Zucchi, A., and Mearini, E. (2006) Overexpression of glyoxalase system enzymes in human kidney tumor. *Cancer J. 12*, 222–228.
26. Schober, R., Buchold, M., Hintersdorf, A., Meixensberger, J., and Birkenmeier, G. (2007) Differential expression of glyoxalase in human brain tumors. *FASEB J. 21*, A27.
27. Padmanabhan, P. K., Mukherjee, A., and Madhubala, R. (2006) Characterization of the gene encoding glyoxalase II from *Leishmania donovanii*: A potential target for anti-parasite drugs. *Biochem. J. 393*, 227–234.
28. Akoachere, M., Iozef, R., Rahlfs, S., Deponte, M., Mannervik, B., Creighton, D. J., Schirmer, H., and Becker, K. (2005) Characterization of the glyoxalases of the malarial parasite *Plasmodium falciparum* and comparison with their human counterparts. *Biol. Chem. 386*, 41–52.
29. Sousa Silva, M., Barata, L., Ferreira, A. E. N., Romao, S., Tomas, A. M., Ponces Freire, A., and Cordeiro, C. (2008) Catalysis and structural properties of *Leishmania infantum* glyoxalase II: Trypanothione specificity and Phylogeny. *Biochemistry 47*, 195–204.
30. Shinohara, M., Thornalley, P. J., Giardino, I., Beisswenger, P., Thorpe, S. R., Onorato, J., and Brownlee, M. (1998) Overexpression of glyoxalase-I in bovine endothelial cells inhibits intracellular advanced glycation endproduct formation and prevents hyperglycemia-induced increases in macromolecular endocytosis. *J. Clin. Invest. 101*, 1142–1147.
31. Chen, F., Wollmer, M. A., Hoerndli, F., Munch, G., Kuhla, B., Rogaev, E. I., Tsolaki, M., Papassotiropoulos, A., and Gotz, J. (2004) Role for glyoxalase I in Alzheimer's disease. *Proc. Natl. Acad. Sci. U.S.A. 101*, 7687–7692.
32. Kuhla, B., Boeck, K., Schmidt, A., Ogunlade, V., Arendt, T., Munch, G., and Luth, H. J. (2007) Age- and stage-dependent glyoxalase I expression and its activity in normal and Alzheimer's disease brains. *Neurobiol. Aging 28*, 29–41.
33. Xu, Y., and Chen, X. (2006) Glyoxalase II, a detoxifying enzyme of glycolysis byproduct methylglyoxal and a target of p63 and p73, is a pro-survival factor of the p53 family. *J. Biol. Chem. 281*, 26702–26713.
34. Marasinghe, G. P. K., Sander, I. M., Bennett, B., Periyannan, G., Yang, K. W., Makaroff, C. A., and Crowder, M. W. (2005) Structural studies on a mitochondrial glyoxalase II. *J. Biol. Chem. 280*, 40668–40675.
35. O'Young, J., Sukdeo, N., and Honek, J. F. (2007) *Escherichia coli* glyoxalase II is a binuclear zinc-dependent metalloenzyme. *Arch. Biochem. Biophys. 459*, 20–26.
36. Talesa, V., Rosi, G., Contenti, S., Mangiabene, C., Lupattelli, M., Norton, S. J., Giovannini, E., and Principato, G. B. (1990) Presence of glyoxalase II in mitochondria from spinach leaves: Comparison with the enzyme from cytosol. *Biochem. Int. 22*, 1115–1120.
37. Oray, B., and Norton, S. J. (1982) Glyoxalase II from mouse liver. *Methods Enzymol. 90*, 547–551.
38. Al-Timari, A., and Douglas, K. T. (1986) Inhibition by glutathione derivatives of bovine liver glyoxalase II (hydroxyacylglutathione hydrolase) as a probe of the N- and S-sites for substrate binding. *Biochim. Biophys. Acta 870*, 219–225.
39. Campos-Bermudez, V. A., Leite, N. R., Krog, R., Costa-Filho, A. J., Soncini, F. C., Oliva, G., and Vila, A. J. (2007) Biochemical and structural characterization of *Salmonella typhimurium* glyoxalase II: New insights into metal ion selectivity. *Biochemistry 46*, 11069–11079.
40. Cameron, A. D., Ridderstrom, M., Olin, B., and Mannervik, B. (1999) Crystal structure of human glyoxalase II and its complex with a glutathione thiolester substrate analogue. *Structure 7*, 1067–1078.
41. Daiyasu, H., Osaka, K., Ishino, Y., and Toh, H. (2001) Expansion of the zinc metallo-hydrolase family of the β-lactamase fold. *FEBS Lett. 503*, 1–6.
42. Aravind, L. (1999) An evolutionary classification of the metallo-β-lactamase fold proteins. *In Silico Biol. 1*, 69–91.
43. Crowder, M. W., Maiti, M. K., Banovic, L., and Makaroff, C. A. (1997) Glyoxalase II from *A. thaliana* requires Zn(II) for catalytic activity. *FEBS Lett. 418*, 351–354.
44. Purpero, V. M., and Moran, G. R. (2006) Catalytic, noncatalytic, and inhibitory phenomena: Kinetic analysis of (4-hydroxyphenyl)-pyruvate dioxygenase from *Arabidopsis thaliana*. *Biochemistry 45*, 6044–6055.
45. Bou-Abdallah, F., and Chasteen, N. D. (2008) Spin concentration measurements of high-spin ($g' = 4.3$) rhombic iron(III) ions in biological samples: Theory and application. *J. Biol. Inorg. Chem. 13*, 15–24.
46. Aasa, R., and Vanngard, T. (1975) EPR signal intensity and powder shapes: A reexamination. *J. Magn. Reson. 19*, 308–315.
47. Crowder, M. W., Yang, K. W., Carenbauer, A. L., Periyannan, G., Seifert, M. A., Rude, N. E., and Walsh, T. R. (2001) The problem of a solvent exposable disulfide when preparing Co(II)-substituted metallo-β-lactamase L1 from *Stenotrophomonas maltophilia*. *J. Biol. Inorg. Chem. 6*, 91–99.
48. Schilling, O., Wenzel, N., Naylor, M., Vogel, A., Crowder, M., Makaroff, C., and Meyer-Klaucke, W. (2003) Flexible metal binding of the metallo-β-lactamase domain: Glyoxalase II incorporates iron, manganese, and zinc *in vivo*. *Biochemistry 42*, 11777–11786.
49. Wenzel, N. F., Carenbauer, A. L., Pfiester, M. P., Schilling, O., Meyer-Klaucke, W., Makaroff, C. A., and Crowder, M. W. (2004) The binding of iron and zinc to glyoxalase II occurs exclusively as dimetal centers and is unique within the metallo-β-lactamase family. *J. Biol. Inorg. Chem. 9*, 429–438.
50. Bebrone, C. (2007) Metallo-β-lactamases (classification, activity, genetic organization, structure, zinc coordination) and their superfamily. *Biochem. Pharmacol. 74*, 1686–1701.
51. Frazao, C., Silva, G., Gomes, C. M., Matias, P., Coelho, R., Sieker, L., Macedo, S., Liu, M. Y., Oliveira, S., Teixeira, M., Xavier, A. V., Rodrigues-Pousada, C., Carrondo, M. A., and Le Gall, J. (2000) Structure of a dioxygen reduction enzyme from *Desulfovibrio gigas*. *Nat. Struct. Biol. 7*, 1041–1045.

52. Uotila, L. (1973) Purification and characterization of S-2-hydroxyacylglutathione hydrolase (glyoxalase II) from human liver. *Biochemistry 12*, 3944–3951.
53. Hu, Z., Periyannan, G., Bennett, B., and Crowder, M. W. (2008) Role of the Zn_1 and Zn_2 sites in metallo-β-lactamase L1. *J. Am. Chem. Soc. 130*, 14207–14216.
54. Hu, Z., Gunasekera, T. S., Spadafora, L., Bennett, B., and Crowder, M. W. (2008) Metal content of metallo-β-lactamase L1 is determined by the bioavailability of metal ions. *Biochemistry 47*, 7947–7953.
55. Orellano, E. G., Girardini, J. E., Cricco, J. A., Ceccarelli, E. A., and Vila, A. J. (1998) Spectroscopic characterization of a binuclear metal site in *Bacillus cereus* β-lactamase II. *Biochemistry 37*, 10173–10180.
56. Williams, R. J. P. (1990) Bioinorganic chemistry: Its conceptual evolution. *Coord. Chem. Rev. 100*, 573–610.
57. Schilling, O., Vogel, A., and Meyer-Klaucke, W. (2001) EXAFS studies on proteins from the metallo-β-lactamase family reveal similar metal sites in an oxido-reductase and the hydrolase ElaC. *J. Inorg. Biochem. 86*, 422.
58. Bennett, B., and Holz, R. C. (1997) Spectroscopically distinct cobalt (II) sites in heterodimetallic forms of the aminopeptidase from *Aeromonas proteolytica*: Characterization of substrate binding. *Biochemistry 36*, 9837–9846.
59. Meijers, R., Adolph, H.-W., Dauter, Z., Wilson, K. S., Lamzin, V. S., and Cedergren-Zeppezauer, E. S. (2007) Structural evidence for a ligand coordination switch in liver alcohol dehydrogenase. *Biochemistry 46*, 5446–5454.
60. Bernstein, H. J. (2000) Recent changes to RasMol, recombining the variants. *Trends Biochem. Sci. 25*, 453–455.